Journal of Organometallic Chemistry 762 (2014) 9–18

Contents lists available at ScienceDirect

Journal of Organometallic Chemistry

journal homepage: www.elsevier.com/locate/jorganchem

# Approaches toward ($\eta^2$-HX) (X = H, SiR (R = $Me_3$ or $Me_2Ph$), $CH_3$) sigma-complexes of ruthenium

K.S. Naidu, Balaji R. Jagirdar*

*Department of Inorganic and Physical Chemistry, Indian Institute of Science, Bangalore 560012, India*

ARTICLE INFO

*Article history:*
Received 11 February 2014
Received in revised form
25 March 2014
Accepted 26 March 2014

*Keywords:*
Lithium tris(pyrazolyl)methane sulfonate
σ–Dihydrogen
σ–Silane
σ–Methane

ABSTRACT

Two new Ru(II)-complexes [RuH(Tpms)($PPh_3$)$_2$] **1** (Tpms = ($C_3H_3N_2$)$_3CSO_3$, tris-(pyrazolyl)methane sulfonate) and [Ru(OTf)(Tpms)($PPh_3$)$_2$] **2** (OTf = $CF_3SO_3$) have been synthesized and characterized wherein Ru–H and Ru–OTf are the key reactive centers. Reaction of **1** with HOTf results in the [Ru($\eta^2$-$H_2$)(Tpms)($PPh_3$)$_2$][OTf] complex **3**, whereas reaction of **1** with $Me_3SiOTf$ affords the dihydrogen complex **3** and complex **1** through an unobserved σ–silane intermediate. In addition, an attempt to characterize the sigma methane complex via reaction of complex **1** with $CH_3OTf$ yields complex **2** and free methane. On the other hand, reaction of [Ru(OTf)(Tpms)($PPh_3$)$_2$] **2** with $H_2$ and $PhMe_2SiH$ at low temperature resulted in σ–$H_2$, **3** and a probable σ–silane complexes, respectively. However, no σ–methane complex was observed for the reaction of complex **2** with methane even at low temperature.



## Introduction

Coordination of an H–X bond (X = H, C, Si) to a transition metal center in an $\eta^2$-fashion, in the so-called σ-complexes has immense importance in the field of catalysis [1–3]. Generally, these σ-complexes are defined as metal complexes containing a ligand in which a σ-bond, H–X (X = H, C, Si, and B) acts as a two-electron donor to the metal center, resulting in a 3 center-2-electron bond [1]. Particularly, the σ–$H_2$ complexes form the best-known group of σ-complexes in which the H–H bond is bound to the metal center in an $\eta^2$-fashion. In addition, several well characterized examples of $\eta^2$-silane and $\eta^2$-borane complexes have also been reported [4]. In recent years, the carbon analogs of these complexes in which alkanes are coordinated through $\eta^2$-C–H bonds to a metal center have been attracting immense attention from the standpoint of organometallic catalysis [5–8].

These σ-complexes are key intermediates in catalytic processes such as hydrogenation, hydrosilylation, hydroboration and alkane functionalization etc. Understanding the nature of the σ-complexes provides an insight into the activation of H–X bonds by transition metal centers. It is also important for fine catalyst design.

Hydrotris(1-pyrazolyl)borate [$HB(pz)_3$, Tp] and its derivative hydrotris(3,5-dimethyl-1-pyrazolyl)borate [$HB(3,5Me_2pz)_3$, Tp′] have been widely explored, however, in comparison, the chemistry of tris(pyrazolyl)methane sulfonate (Tpms)-transition metal complexes has been far less developed [9]. The Tpms bears a methanesulfonate anionic moiety, which imparts very good stability toward hydrolysis and an increased solubility in polar solvents [10]. It is a very good chelating tripodal ligand and shows dynamic $\kappa^2$ and $\kappa^3$ modes of coordination. In addition, it behaves as a flexidentate NNN and NNO donor, depending on the nature of the complex [11]. This versatile behavior of the Tpms ligand, motivated us to explore the chemistry of ruthenium complexes for σ-bond activation; to our knowledge, very few results on C–H bond activation of benzene by metal complexes bearing the Tpms ligand are reported [12,13].

Several synthetic methods are available to obtain σ-complexes. For example, coordinatively unsaturated complexes or complexes having highly labile groups react with H–X (X = H, C, Si, and B) σ–donor ligand resulting in the formation of σ-complexes. Another approach involves reaction of metal-hydride ([M]–H) complexes with electrophiles such as HOTf, $CH_3OTf$, and $Me_3SiOTf$ to lead to formation of σ-complexes. In addition, metal-alkyl (or silyl) complexes also react with $H^+$ to form σ-complexes [14,15]. However, limited examples of metal complexes that can stabilize all three σ-donor ligands (H–H, Si–H, and C–H) have been reported; e.g., Kubas and co-workers reported a metal complex wherein Si–H, H–H, and agostic C–H bonds are bound to the same metal fragment in an $\eta^2$ fashion [16]. In order to widen the scope of these studies and to gain more insight into the bonding nature and reactivity behavior of σ-$H_2$, silane and methane complexes, we employed two strategies to obtain these complexes in solution. In the first, reactions of [RuH(Tpms)($PPh_3$)$_2$], **1** (Tpms = tris(pyrazolyl)methane sulfonate) with electrophilic reagents such as HOTf, $Me_3SiOTf$, and $CH_3OTf$ and in the second strategy, reactions of [Ru(OTf)(Tpms)($PPh_3$)$_2$] (OTf = $CF_3SO_3$), **2** with $H_2$, $PhMe_2SiH$, and $CH_4$ (at 7 bar) at low temperature were carried out. Herein, we describe these reactions in detail.

* Corresponding author.
*E-mail address:* jagirdar@ipc.iisc.ernet.in (B.R. Jagirdar).

http://dx.doi.org/10.1016/j.jorganchem.2014.03.027
0022-328X/

## Results and discussion

*Synthesis and characterization of [RuH(Tpms)(PPh$_3$)$_2$], **1** and [Ru(OTf)(Tpms)(PPh$_3$)$_2$], **2** complexes*

Reaction of [RuH$_2$(PPh$_3$)$_4$] with LiTpms produced the yellow monohydride complex [RuH(Tpms)(PPh$_3$)$_2$] (eq (1)). Upon workup and crystallization in $CH_2Cl_2$–n-hexane solutions, yellow crystals of the complex were obtained in 50% yield. The $^1$H NMR spectrum of **1** shows a triplet for the hydride at $\delta$ −13.35 due to coupling with 2 equivalent cis phosphorus nuclei with a $J$(H,P$_{cis}$) of 27.7 Hz. The Tp analog [RuH(Tp)(PPh$_3$)$_2$], reported by Lau and Jia exhibits very similar NMR spectral features [17]. The $^{31}$P{$^1$H} NMR spectrum is composed of only one singlet at $\delta$ 65.8, indicating the *cis* disposition of the two phosphines.

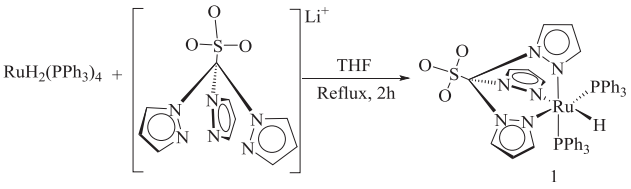


(1)

We also found that in dichloromethane, complex **1** slowly undergoes hydride chloride exchange in days. In an attempt to prepare a five coordinate [Ru(Tpms)(PPh$_3$)$_2$][OTf] complex from [Ru(Cl)(Tpms)(PPh$_3$)$_2$], we used AgOTf for the abstraction of chloride. Because of the high instability of the putative five coordinate species upon chloride abstraction, it immediately reacts with the triflate anion and affords [Ru(OTf)(Tpms)(PPh$_3$)$_2$], complex **2** (eq (2)). Formation of complex **2** was evidenced by NMR spectroscopy and X-ray crystallography. This product was crystallized from a dichloromethane solution via slow diffusion of petroleum ether at room temperature over a period of 2 days; yellow crystals were obtained in 80% yield. Complex **2** is moderately soluble in toluene, THF and completely soluble in chlorinated solvents. $^{19}$F NMR spectrum confirmed the presence of a coordinated triflate ligand. In particular, $^{19}$F NMR spectrum of **2** exhibits a singlet for $CF_3$ at $\delta$ −76.6 ppm, downfield from free triflate ion ($\delta$ −79.0 ppm). The $^{31}$P{$^1$H} NMR spectrum displays a single peak at $\delta$ 36.6 ppm indicating the *cis* disposition of the two equivalent phosphines.

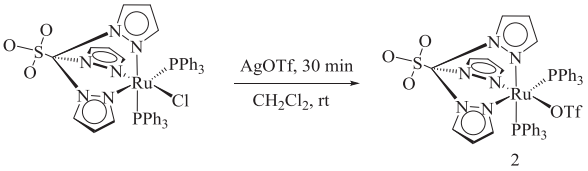


(2)

*Protonation of [RuH(Tpms)(PPh$_3$)$_2$]*

We carried out protonation of the monohydride complex, [RuH(Tpms)(PPh$_3$)$_2$] with HOTf in dichloromethane which resulted in the molecular hydrogen complex [Ru($\eta^2$-H$_2$)(Tpms)(PPh$_3$)$_2$][OTf], **3** at low temperature (243 K) (eq (3)). The existence of the $\eta^2$-H$_2$ moiety in **3** was confirmed by variable-temperature spin-lattice relaxation time measurements $T_1$ and the observation of a large $^1J$(H,D) for the corresponding isotopomer [Ru(HD)(Tpms)(PPh$_3$)$_2$][OTf], **3-$d_1$**. The $^1$H NMR spectrum of **3** in $CD_2Cl_2$ showed a broad signal at $\delta$ −7.63 ppm integrating to two hydrogen atoms. A $T_1$ (min) value of 15.8 ms (400 MHz) was obtained for the broad signal at −7.63 ppm at 243 K. The H–H distances $d_{HH}$ can be calculated from the $T_1$ (min) value [18] and are 1.08 and 0.85 Å for slow and fast rotation regimes of the bound $H_2$ in **3**. More definitive evidence for the intact nature of the H–H bond in these derivatives was obtained from the $J$(H,D) coupling for the HD isotopomer. We purged the $CD_2Cl_2$ solution containing the [Ru($\eta^2$-H$_2$)(Tpms)(PPh$_3$)$_2$][OTf] complex with HD gas (generated from NaH and $D_2O$) at 243 K, which gave the $\eta^2$-HD isotopomer [Ru($\eta^2$-HD)(Tpms)(PPh$_3$)$_2$][OTf]; it showed a 1:1:1 triplet ($^1J$(HD) = 31.6 Hz) of a 1:2:1 triplet ($^2J$(HP) = 6.6 Hz) centered at $\delta$ −7.63 ppm in the $^1$H NMR spectrum, after nullifying the $\eta^2$-H$_2$ peak at $\delta$ −7.63 ppm by using the inversion-recovery method with a delay time of 11 ms. The H–H distance ($d_{HH}$) calculated from the inverse relationship between $d_{HH}$ and $J$(H,D) of the HD isotopomer [19,20] is 0.86 Å (see Supporting information) which closely corresponds to the value calculated from $T_1$ for rapidly rotating $H_2$. Dihydrogen complex **3** was found to be labile at room temperature; the bound $H_2$ gets replaced by the counter anion OTf and leads to the formation of [Ru(OTf)(Tpms)(PPh$_3$)$_2$].

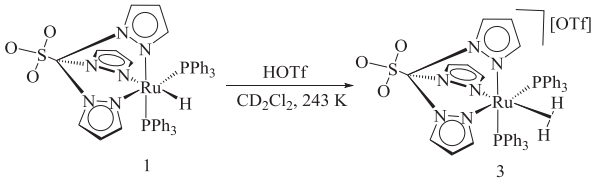


(3)

*Reaction of [RuH(Tpms)(PPh$_3$)$_2$], **1** with Me$_3$SiOTf*

In an attempt to obtain a ruthenium $\eta^2$–silane complex, we treated complex **1** with Me$_3$SiOTf and monitored the reaction using NMR spectroscopy. In this reaction at 193 K, instead of cationic $\eta^2$–silane intermediate we observed peaks corresponding to the dihydrogen complex **3** and hydride complex **1** (Scheme 1). On the basis of these products we propose that the electrophile $Me_3Si^+$ attacks complex **1** and forms a highly electrophilic unobservable cationic [Ru($\eta^2$-HSiMe$_3$)(Tpms)(PPh$_3$)$_2$][OTf] species. This species rapidly undergoes hydrolysis due to the presence of residual water in the solvent and forms dihydrogen complex **3** and Me$_3$SiOH (Scheme 1). Brookhart and his co-workers [15] noted that cationic $\eta^2$–silane complexes are quite sensitive to weak nucleophiles or even non-nucleophilic counter ions such as $BF_4^-$, resulting in the formation of R$_3$SiF. Closely related system, for example, [Fe(Cp)($\eta^2$-HSiEt$_3$)(CO)(PEt$_3$)][BF$_4$] is readily hydrolyzed by trace amount of water and forms Et$_3$SiOH and [Fe($\eta^2$-H$_2$)(Cp)(CO)(PEt$_3$)][BF$_4$] [21]. The appearance of a broad singlet at $\delta$ −7.63 ppm in the $^1$H NMR spectrum and a singlet at $\delta$ 43.6 ppm in the $^{31}$P{$^1$H} NMR spectrum are consistent with the dihydrogen complex [Ru($\eta^2$-H$_2$)(Tpms)(PPh$_3$)$_2$][OTf], **3** all other signals of complex **3** were also observed and matched those of an authentic sample. In addition, Me$_3$SiOH shows a singlet at $\delta$ 0.05 ppm for methyl protons in the $^1$H NMR spectrum (Fig. 1). Another possibility is that the electrophilic reagent reacts first with the water present in the solvent to generate HOTf, which causes the protonation of the hydride complex to form the dihydrogen complex **3** (see Supplementary material). In order to trace generation of HOTf, we carried out an independent reaction; reaction of Me$_3$SiOTf and water leads to the

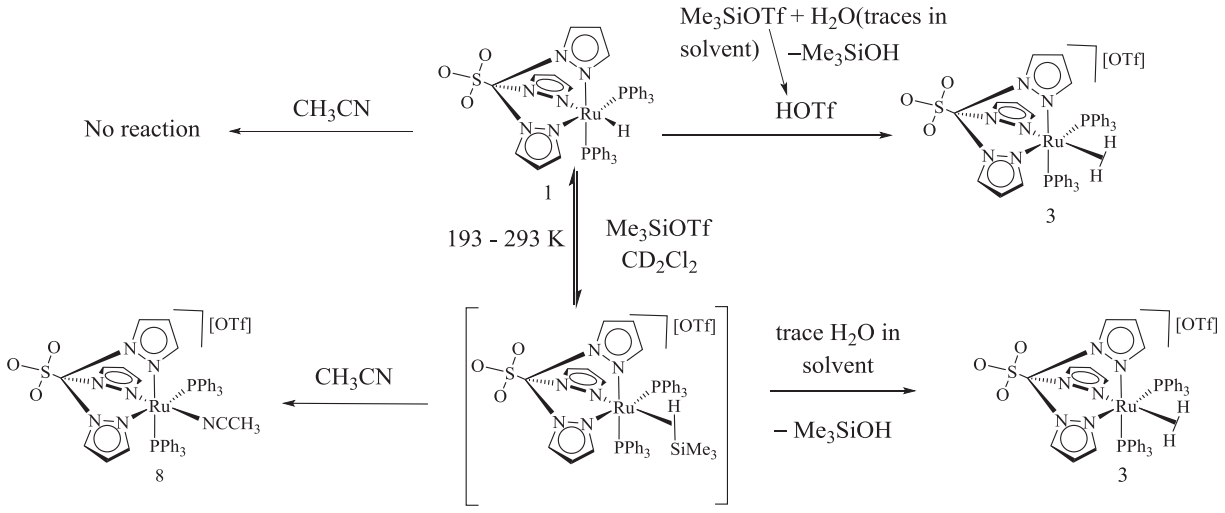


**Scheme 1.** Reaction of complex **1** with $Me_3SiOTf$.

formation of HOTf (see Supplementary material). On the other hand, cationic silane intermediate could also undergo nucleophilic attack by counter ion OTf, leading to the formation of **1** and $Me_3SiOTf$. Identification of methyl signals in the NMR spectrum for the eliminated $Me_3SiOTf$ was difficult due to excess $Me_3SiOTf$ present in the reaction mixture. As is evident from the $^1H$ NMR spectral stack plot, the signal of the dihydrogen complex **3** remained intact up to 273 K and due to lower thermal stability of **3** at higher temperature (293 K) it eliminates $H_2$ and forms complex **2** (see Supplementary material). Formation of complex **3** even at low temperature is indicative of the highly reactive nature of the cationic σ–silane intermediate which undergoes Si–H bond cleavage by weak nucleophiles such as residual water.

From the VT $^1H$ NMR spectral stack plot it is apparent that (Fig. 1), the starting materials (complex **1** and $Me_3SiOTf$) were present throughout the temperature range (193–293 K). Another possibility is that there is no reaction between complex **1** and $Me_3SiOTf$. To rule out this possibility, we carried out two independent reactions of complex **1** (see Supplementary material). In the first reaction, complex **1** was treated with acetonitrile, however no reaction took place. In the second reaction, acetonitrile was added to the solution of complex **1** and $Me_3SiOTf$ in dichloromethane; in this case, we observed complete conversion of the hydride complex **1** to acetonitrile complex $[Ru(NCCH_3)(Tpms)(PPh_3)_2][OTf]$, **8**. These observations suggest that $Me_3Si^+$ electrophile attacks the hydride complex and forms the highly electrophilic cationic $[Ru(\eta^2\text{-}HSiMe_3)(Tpms)(PPh_3)_2][OTf]$ sigma silane complex. To this solution, addition of acetonitrile results in elimination of free silane which is observed in the NMR when acetonitrile substitutes for the silane. Whereas, in the absence of acetonitrile, $OTf^-$ acts as a nucleophile and brings about the Si–H bond cleavage leading to the formation of hydride complex **1**.

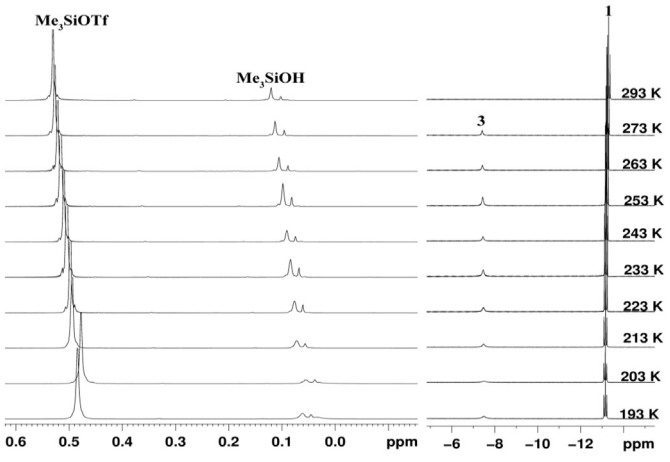


**Fig. 1.** VT $^1H$ NMR spectral stack plot for the reaction of $[RuH(Tpms)(PPh_3)_2]$ with $Me_3SiOTf$.

*Attempt to prepare $[Ru(\eta^2\text{-}CH_4)(Tpms)(PPh_3)_2][OTf]$*

Brookhart and co-workers reported solution state NMR characterization of sigma methane complex $[(PONOP)Rh(CH_4)]^+$ at −110 °C which strengthen our understanding of the binding of the C–H bond of methane and its activation [6]. Recently, Weller et al. characterized rhodium(I) σ–alkane complex in the solid state [8]. In addition, Perutz and co-workers reported Mn–propane and Mn–butane σ–alkane complexes of $[MnCp(CO)_2]$ fragment which was generated in situ from $[MnCp(CO)_3]$ photochemically at low temperature with alkane as solvent [22]. Moreover, Ball and his group recently reported the $[(L_{OEt})Re(CO)_2(alkane)]$ (alkane = cyclopentane, cyclohexane, pentane; $L_{OEt}$ = cyclopentadienyltris(diethyl-phosphito)cobaltate(III)) species using both IR and NMR spectroscopies [23]. These results extend the range of alkane complexes observable by NMR spectroscopy.

Following the Brookhart's strategy, we attempted to generate methane ligand directly bound in the coordination sphere of the ruthenium metal by treating electrophilic reagent ($CH_3OTf$ or $CD_3OTf$) with hydride $[RuH(Tpms)(PPh_3)_2]$ (Scheme 2). We found that the reaction was quite slow at low temperature (203 K), however, at 213 K complex **1** started reacting and eliminates $CH_4$ (or $CD_3H$) accompanied by the formation of complex **2**. The sigma methane intermediate was not observed even after ~2 h at 213 K. We noted signals for $CH_4$ and $CD_3H$ at δ, 0.18 and 0.16 ppm, respectively in the $^1H$ NMR spectra. In addition, $^{31}P\{^1H\}$ NMR spectrum shows a peak at δ 36.5 ppm for complex **2** (see Supplementary material). Other minor products were $[Ru(\eta^2\text{-}H_2)(Tpms)(PPh_3)_2][OTf]$ (**3**) and $[Ru(H_2O)(Tpms)(PPh_3)_2][OTf]$ (**6**). The possible pathway for the generation of these minor products is through the hydrolysis of $CH_3OTf$ by residual water which generates HOTf which in turn protonates complex **1** and leads to the

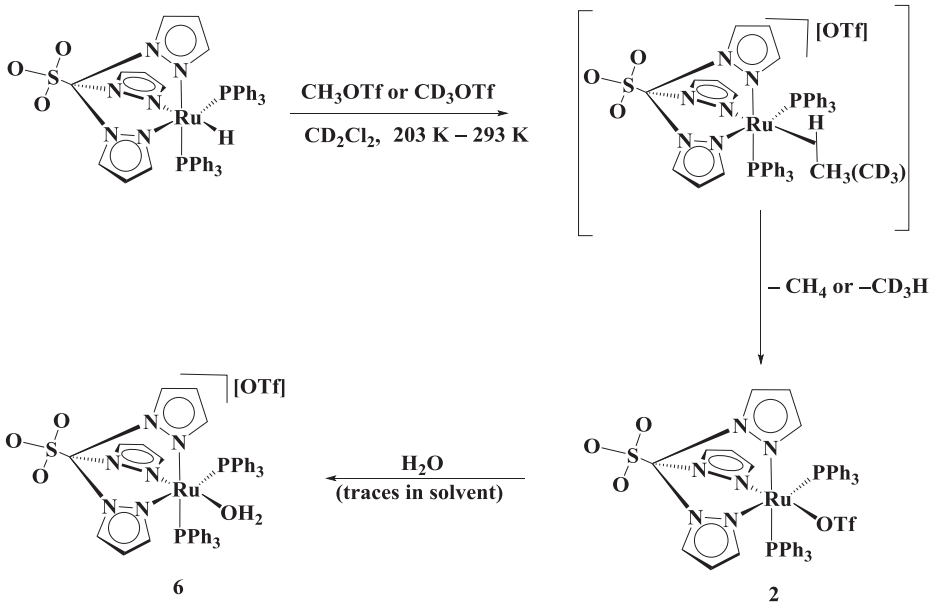


**Scheme 2.**

formation of complex **3**. $^{31}P\{^1H\}$ NMR spectral stack plot (see Supplementary material) suggests that complex **6** is formed through complex **2**. Even trace amount of moisture in rigorously dried solvent causes the formation of the aqua complex. Since alkanes and in particular methane, are very poor electron donors and acceptors, bind rather quite weakly to metal centers. Stronger binding ability of OTf compared to $CH_4$ or $CD_3H$ rendered the formation and observation of only the triflate complex but not the methane complex.

*Reaction of [Ru(OTf)(Tpms)(PPh$_3$)$_2$] with H$_2$*

In the case of protonation reaction of complex **1** with HOTf, we noted that complex **3** to be quite unstable at room temperature and resulted in the formation of complex **2** and evolution of free $H_2$ over ~10 min. However, complex **3** was found to be stable enough and $H_2$ was bound intact to the metal center at low temperature (243 K), and no free $H_2$ was observed. In an attempt to observe complex **3** at RT, complex **2** was pressurized with 1 or 2 bar of $H_2$ at 298 K which resulted in the formation of a small amount of dihydrogen complex [Ru($\eta^2$-$H_2$)(Tpms)($PPh_3$)$_2$][OTf] (**3**) (Scheme 4) via the displacement of the weakly bound OTf ion (see Supplementary material). This indicates that $H_2$ is not a better donor than OTf at room temperature.

*Reaction of [Ru(OTf)(Tpms)(PPh$_3$)$_2$] with PhMe$_2$SiH*

Reaction of [Ru(OTf)(Tpms)($PPh_3$)$_2$] (**2**) with $PhMe_2SiH$ at room temperature resulted in the formation of [RuH(Tpms)($PPh_3$)$_2$] (**1**), [Ru(Tpms)($PPh_3$)($\eta^3$-$HSiMe_2Ph$)] (**4**), [RuCl(Tpms)($PPh_3$)$_2$] (**7**) complexes and $PhMe_2SiOH$, $PhMe_2SiOTf$ and [$PPh_3SiMe_2Ph$][OTf] as evidenced by NMR spectroscopy (Scheme 3). This reaction was found to be slow and took ~24 h at room temperature to reach completion. The spectral properties of **1**, **4** and **7** matched those of similar complexes reported in the literature [24,25] (see Supplementary material). In order to get an insight into the mechanistic aspects of the reaction, we carried out the same reaction at low temperature and monitored the progress of the reaction by using VT NMR spectroscopy. The VT partial $^1H$ NMR spectral stack plot of this reaction is shown in Fig. 2 and the corresponding $^{31}P\{^1H\}$ NMR spectral stack plot has been deposited in the Supplementary material.

Complex **2** contains a triflate, which is bound to the ruthenium center opposite to one of the nitrogen atoms of the pyrazole of Tpms ligand. Generally, silanes are good sigma donors when compared to the H–H and C–H moieties [26]. In this reaction Si–H bond of $HSiMe_2Ph$ could replace the weakly coordinating triflate to form highly reactive cationic intermediate [Ru(Tpms)($PPh_3$)$_2$($\eta^2$-$HSiMe_2Ph$)][OTf] **2.1** (see Scheme 4). It is well established that labile ligands in transition metal complexes can be displaced by free silanes to form $\eta^2$-silane complexes [21]. The $^1H$ NMR spectral data displayed a low intensity broad singlet at −6.21 ppm and the $^{31}P\{^1H\}$ NMR showed a signal at 47.2 ppm. These signals could be due to the $\eta^2$-silane species **2.1** at 253 K. Appearance of a broad signal is indicative of rapid exchange of coordinated silane with triflate in the temperature range 253–223 K. Mechanistically, these reactions may proceed via two main pathways. The first pathway wherein intermediate species **2.1** undergoes rapid hydrolysis of Si–H bond

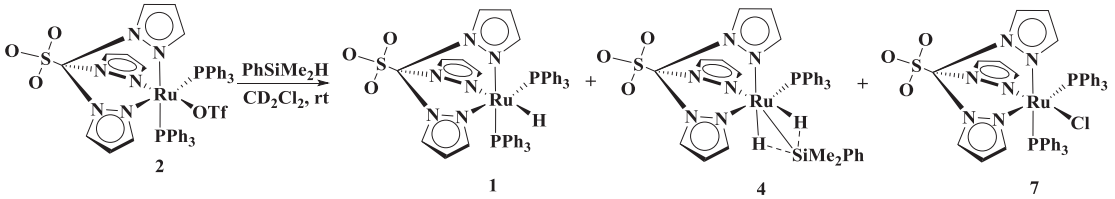


**Scheme 3.**

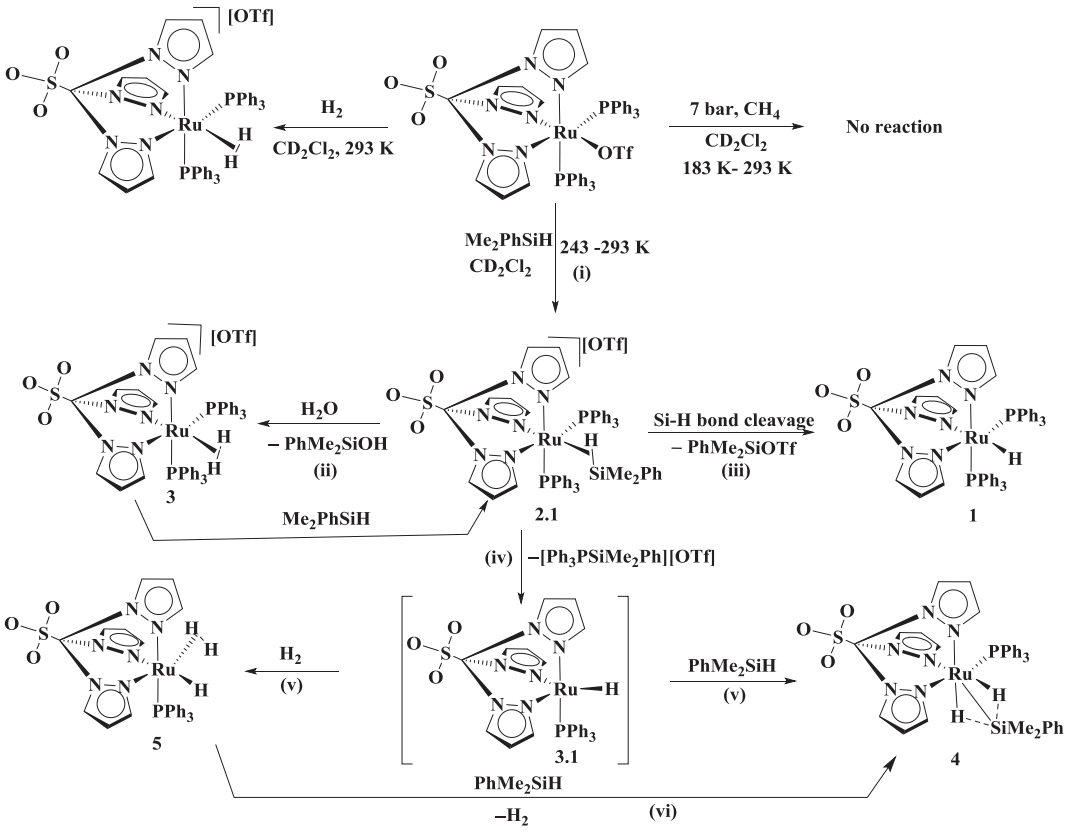


**Scheme 4.** Proposed mechanism of the reaction of complex **2** with $PhMe_2SiH$.

due to the presence of residual water, leads to $H_2$ gas evolution and $PhMe_2SiOH$ formation. This process would take place until complete consumption of residual water present in the solvent. At the same time, very small amount of aqua complex **6** present in the starting material also assists the hydrolysis of free silane via an intermediate **2.1** and forms $H_2$ and $PhMe_2SiOH$. The hydrolysis products $H_2$ gas and $PhMe_2SiOH$ were noted in the $^1H$ NMR spectrum as a singlet at $\delta$ 4.6 ppm and another singlet at 0.3 ppm for methyl protons of $PhMe_2SiOH$ (see Supplementary material). Free $H_2$ generated in the reaction gets consumed by complex **2** giving rise to **3** as noted above. The appearance of a broad singlet at $\delta$ −7.63 ppm and singlet at $\delta$ 43.6 ppm in the $^1H$ and $^{31}P\{^1H\}$ NMR spectra, respectively are consistent with the dihydrogen complex **3**. In order to understand the origin of $H_2$, we carried out few independent reactions; reaction of $PhMe_2SiH$ with residual water in $CD_2Cl_2$ leads to no $H_2$ evolution and silane hydrolysis even up to ~2 h. Once we add complex **2** to this solution, we noted instantaneous liberation of $H_2$ (signal at $\delta$ 4.6 ppm in $^1H$ NMR spectrum), along with $Me_2PhSiOH$ (see Supplementary material). This indicates an important role of complex **2** in the initiation of metal complex assisted silane hydrolysis. Attempts to avoid all traces of water from $CD_2C1_2$ and $PhMe_2SiH$ to protect the cationic silane intermediate **2.1** from hydrolysis were unsuccessful. Wide variety of neutral transition metal sigma silane complexes have been extensively studied although the cationic complex of type **2.1** is limited due to its remarkable reactivity toward water and attack of weakly coordinating anions such as $BF_4$, OTf [15,27]. In the other pathway, the intermediate **2.1** rapidly undergoes Si–H bond cleavage by weakly coordinating counter anion OTf to afford hydride derivative $[RuH(Tpms)(PPh_3)_2]$, **1** and $PhMe_2SiOTf$ as observed in the NMR spectra. More importantly, from the $^1H$ NMR spectral stack plot we noted that hydrolysis was much more rapid in comparison to Si–H bond cleavage by counter anion OTf which could be due to the better nucleophilicity of water than that of OTf. The Si–H bond cleaved product, $PhMe_2SiOTf$ was noted in the $^1H$ NMR spectrum as a singlet at $\delta$ 0.7 ppm for methyl groups. There have been limited reports in the literature about heterolytic cleavage of SiH bond, in which a σ-complex was observed as an intermediate in the activation pathway [15,21,28]. Upon raising the temperature of the reaction to 268 K, the spectral stack plots (Fig. 2) show complexes **4** and **5** along with formation of $[PPh_3SiMe_2Ph][OTf]$ species. Complex **4** shows a doublet at $\delta$ −11.21 ppm (Ru-$\eta^3$-

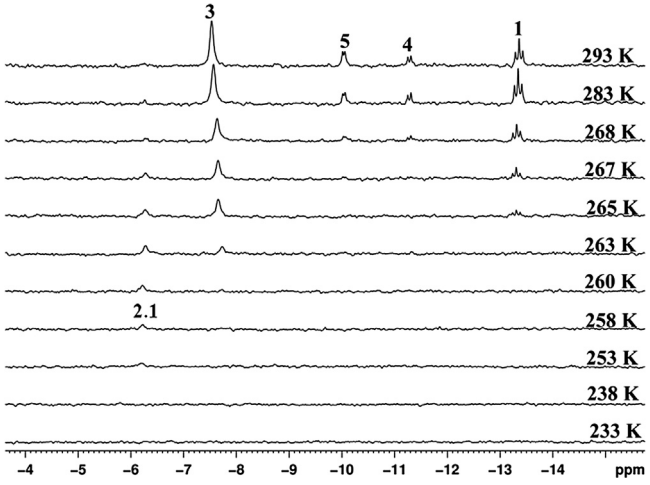


**Fig. 2.** VT $^1H$ NMR spectral stack plot with temperature showing complexes **1**, **3**, **4** and **5** in the reaction of complex **2** with $PhMe_2SiH$ in $CD_2Cl_2$.

$H_2SiMe_2Ph$) which integrates to two protons in the $^1H$ NMR spectrum; the doublet is flanked by $^{29}Si$ satellite signals $J(SiH) = 22$ Hz indicating the presence of $\eta^2$-silane ligand and a sharp singlet at $\delta$ 69.9 ppm in the $^{31}P\{^1H\}$ NMR spectrum. Similar complex of **4** with Tp ligand was reported by Lau et al. by reacting $[TpRuH(CH_3CN)(PPh_3)]$ with $PhMe_2SiH$ at 90 °C for 4 h [24]. In addition, complex **5** shows a doublet at $\delta$ −10.11 ppm (RuH-$\eta^2$-$H_2$) in the $^1H$ NMR spectrum and a sharp singlet at $\delta$ 70.19 ppm in the $^{31}P\{^1H\}$ NMR spectrum. The value of $J(HP) = 18$ Hz and the peak nature for the dihydrogen complex can be compared with the analogous $[TpRuH(\eta^2\text{-}H_2)(PPh_3)]$ complex [29]. It might be that complex **2.1** undergoes subsequent intramolecular dissociation of $[PPh_3SiMe_2Ph][OTf]$ (Scheme 4) and formation of unobserved complex [RuH(Tpms)($PPh_3$)], **3.1**. In this reaction, the in-situ formation of $[PPh_3SiMe_2Ph][OTf]$ was not observed in the NMR spectrum at low temperature because of its poor solubility. However at room temperature, the $^1H$ NMR spectrum of $[PPh_3SiMe_2Ph][OTf]$ shows a doublet at 2.78 ppm and the $^{31}P\{^1H\}$ NMR spectrum displayed a signal at 21.2 ppm, which was further confirmed by HSQC of $^1H-^{31}P$ NMR spectrum (see Supplementary material). A similar observation on the intramolecular dissociation was reported wherein Si–H bond gets cleaved at the metal center with elimination of Si–OH species [24]. Based on NMR spectral evidence, it could be envisioned that formation of complexes **4** and **5** take place via the intermediacy of a highly reactive five coordinated neutral complex **3.1**; this species could be a very short lived one and reacts instantaneously with $PhMe_2SiH$ and free $H_2$ present in the solution. Apparently, we noted that the major product was **4** compared to **5** because it can also react with free silane ($PhMe_2SiH$) present in the solution to form **4**. Additionally, to rule out the possibility of formation of **4** and **5** via **1**, we independently established the reaction of **1** with $PhMe_2SiH$ at room temperature and found that formation of a small amount of **4** and free $PPh_3$ take place after one week (see Supplementary material). On the other hand, complex **3** is unstable at room temperature and slowly goes back to $[Ru(OTf)(Tpms)(PPh_3)_2]$ within a short time (~10 min). Another plausible route for the formation of complex **3** is that $H_2$ could be substituted by $PhMe_2SiH$ to give **2.1** (as mentioned earlier, silane is a better donor than $H_2$). Complex **1** is reactive toward $CD_2Cl_2$ to form $[RuCl(Tpms)(PPh_3)_2]$, **7** through a metathesis process. Complex **7** shows a sharp singlet at 37.5 ppm in the $^{31}P\{^1H\}$ NMR spectrum.

*Attempted preparation of sigma methane complex from [Ru(OTf)(Tpms)(PPh$_3$)$_2$] and CH$_4$ at 7 bar*

The lability of triflate in complex **2** is clearly demonstrated by its reaction with acetonitrile and water which results in the formation of $[Ru(NCCH_3)(Tpms)(PPh_3)_2][OTf]$, **8** and $[Ru(H_2O)(Tpms)(PPh_3)_2][OTf]$, **6** complexes, respectively. Structures for these two complexes were determined unambiguously by X-ray crystallography (Figs. 5 and 6). We found that in complex **2** the Ru–O bond distance is 2.198(2) Å, which is indicative of weakly coordinating nature of the triflate ion. Generally, weakly coordinating triflate ion is expected to be a better leaving group in presence of strong donors such as acetonitrile and water as mentioned earlier; however, for very weakly coordinating ligands especially C–H bond of simple alkanes, triflate behaves as strong ligand and remains tightly bound to the metal center as we observed this when **2** was reacted with $CH_4$ at 7 bar. On the other hand, the reactions of complex **2** with $H_2$ and $PhMe_2SiH$, resulted in a σ–$H_2$ complex (**3**) and Si–H bond activation along with silane hydrolysis through an expected σ–silane intermediate **2a**, respectively. As in the case of $H_2$ and silane reactions of complex **2**, methane complexation with **2** at low temperature and 7 bar of $CH_4$ could be possible. In this context, we

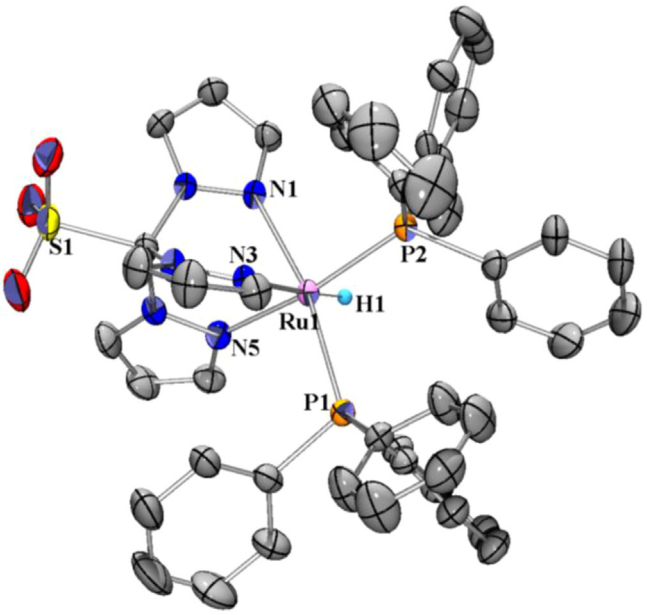


**Fig. 3.** ORTEP view of $[RuH(Tpms)(PPh_3)_2]$ complex, **1** at the 50% probability level showing selected atom labeling. Hydrogen atoms are omitted for clarity except for the hydride H1.

pressurized complex **2** with 7 bar of $CH_4$ at 298 K (Scheme 4), and the reaction was monitored by VT NMR spectroscopy. We gradually cooled down the NMR probe from 293 K to 183 K (see Supplementary material). However, under these conditions even at 183 K, we did not observe any signal for a σ–methane complex spectroscopically. The sample was kept at 183 K for nearly 3 h to find any trace amount of σ–methane complex formed in solution; however no signals were found. On the other hand, broadening of the $^{31}P\{^1H\}$ NMR spectral signal was noted at 203–213 K along with change in the pattern of proton signals of the aromatic region. Then further cooling led to disappearance of the $^{31}P\{^1H\}$ NMR spectral

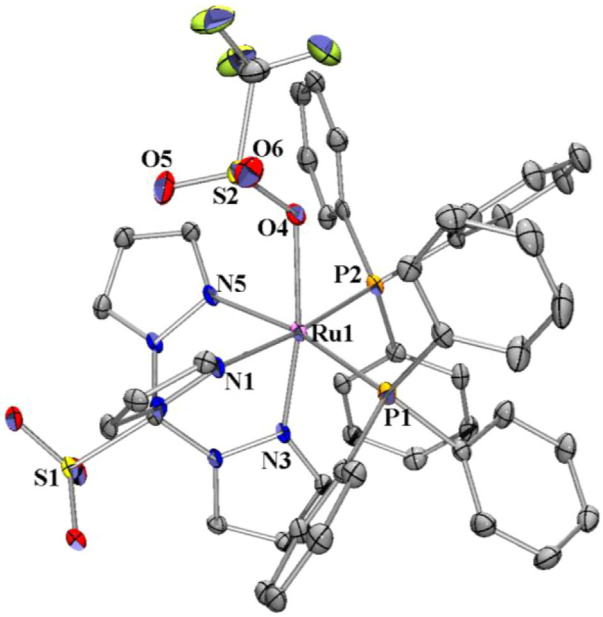


**Fig. 4.** ORTEP view of $[Ru(OTf)(Tpms)(PPh_3)_2]$ complex, **2** at the 50% probability level showing selected atom labeling. Hydrogen atoms are omitted for clarity.

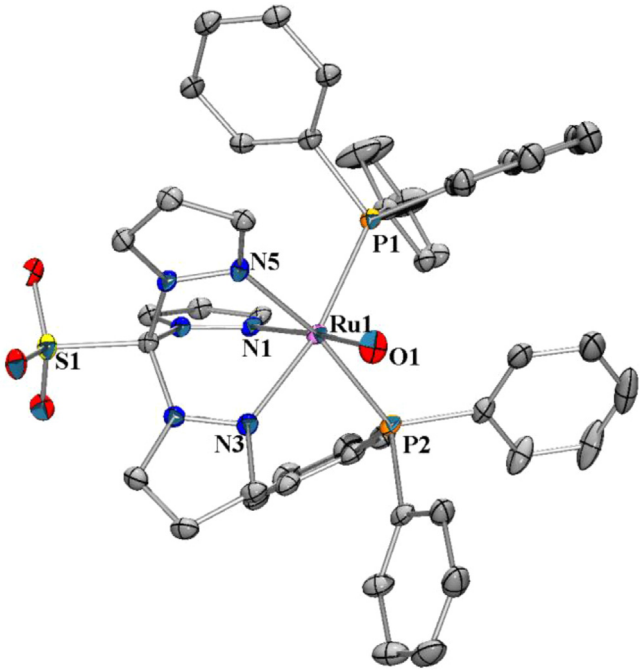


**Fig. 5.** ORTEP view of $[Ru(H_2O)(Tpms)(PPh_3)_2]$ complex, **6** at the 50% probability level showing selected atom labeling. Hydrogen atoms are omitted for clarity.

signal and reappearance of two separate broad signals at 183 K, and again a clear change in the pattern of proton signals of aromatic region at 183 K (see Supplementary material) which could be due to weak interactions of phenyl protons of $PPh_3$ competing with triflate counter anion for binding at the metal center at low temperature which are in rapid equilibrium.

$H_2$ and silane are better donors as compared to methane wherein $H_2$ and silane σ-binding to metal center are governed by electron donation from σ–H–H and Si–H bonds to metal and the π-back bonding from metal to the respective σ* orbitals of these ligands. In contrast, alkanes especially methane, notoriously unreactive, interact with metals very weakly because the HOMO (σ) is low-lying and therefore, unsuitable for electron donation, and the LUMO (σ*) is high in energy and unsuitable for accepting electron density and in addition, the dominant coordinating ability of OTf in comparison to the weakly coordinating nature of methane, could be the two reasons for not being able to observe interaction of methane with complex **2**.

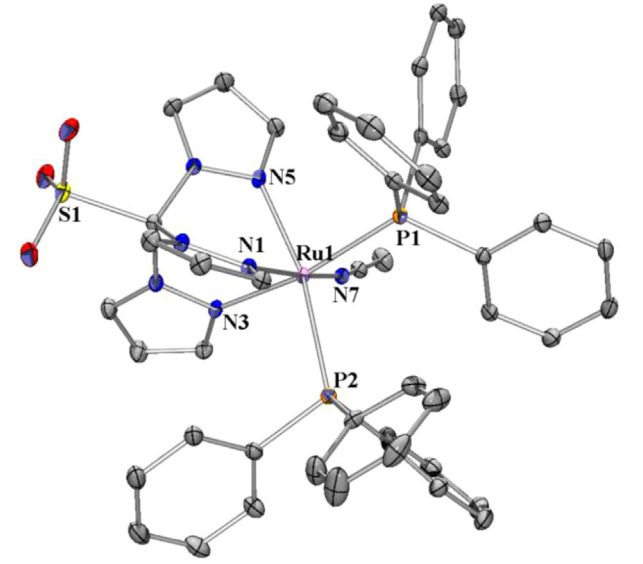


**Fig. 6.** ORTEP view of $[Ru(CH_3CN)(Tpms)(PPh_3)_2]$ complex, **8** at the 50% probability level showing selected atom labeling. Hydrogen atoms are omitted for clarity.

**Table 1**
Selected bond distances (Å) and angles (°) for complexes **1**, **2**, **6** and **8**.

| | 1 | 2 | 6 | 8 |
|---|---|---|---|---|
| Ru1–[a]L′ | 1.58(3) | 2.198(2) | 2.126(3) | 2.0319(16) |
| Ru1–N1 | 2.154(2) | 2.077(2) | 2.039(3) | 2.0688(16) |
| Ru1–N3 | 2.1628(19) | 2.029(2) | 2.125(3) | 2.0967(16) |
| Ru1–N5 | 2.116(2) | 2.104(2) | 2.099(3) | 2.1214(16) |
| Ru1–P1 | 2.3169(8) | 2.4037(8) | 2.3856(9) | 2.3739(5) |
| Ru1–P2 | 2.2910(9) | 2.3858(8) | 2.3646(9) | 2.3946(5) |
| P2–Ru1–P1 | 100.02(3) | 99.71(3) | 101.84(3) | 101.086(17) |
| N1–Ru1–N3 | 82.10(8) | 85.48(9) | 85.62(12) | 86.74(6) |
| P2–Ru1-L′ | 84.2(12) | 89.26(6) | 91.19(9) | 97.19(5) |
| N3–Ru1-L′ | 173.8(12) | 170.17(8) | 86.38(12) | 87.93(6) |
| N1–Ru1–P2 | 92.09(6) | 172.94(7) | 94.63(8) | 88.59(4) |

[a] L′ represents the atom of the monodentate ligand coordinated to Ru, L′ = H (**1**), OTf (**2**), $H_2O$ (**6**), $CH_3CN$ (**8**).

### *X-ray structural studies of **1**, **2**, **6** and **8***

Molecular structures of **1**, **2**, **6** and **8** have been confirmed by an X-ray crystallographic study. The molecular geometries of **1**, **2**, **6** and **8** are depicted in Figs. 3–6 and the crystallographic details and selected bond distances and angles have been summarized in Tables 1 and 2. The geometries of these four structures were found to be quite similar to one another. The ruthenium center in all these structures adopts an approximately octahedral geometry, with the Tpms ligand occupying one face of the octahedron and the phosphines and L′ (L′ = H, OTf, $H_2O$, $NCCH_3$) ligands occupying the remaining positions. The Ru–N distance (L′ *trans* to N of pyrazolyl) in **1** was found to be slightly longer (2.1628(19) Å) in comparison to the other three (2.029(2) Å), (2.039(3) Å), (2.0688(16) Å); **2**, **6**, **8**, respectively structures which could be attributed to the good sigma donating ability of the hydride ligand *trans* to N. The distances between the ruthenium atom and the metal bound pyrazolyl nitrogen atoms in all these structures compare well with those

**Table 2**
Crystal data and refinement details for **1**, **2**, **6**, **8**.

| | 1 | 2 | 6 | 8 |
|---|---|---|---|---|
| Formula | $C_{47}H_{45}Cl_2N_6O_3P_2RuS$ | $C_{49}H_{43}Cl_4F_3N_6O_6P_2RuS_2$ | $C_{48}H_{41}Cl_2F_3N_6O_9P_2RuS_2$ | $C_{60}H_{58}F_3N_7O_8P_2RuS_2$ |
| Formula weight | 1004.84 | 1237.82 | 1200.92 | 1289.26 |
| Cryst syst | Triclinic | Triclinic | Triclinic | Triclinic |
| Space group | $P-1$ | $P-1$ | $P-1$ | $P-1$ |
| $T$ (K) | 293(2) | 100(2) | 100(2) | 100(2) |
| $a$, Å | 12.236(5) | 11.4609(10) | 11.7928(5) | 12.0652(7) |
| $b$, Å | 13.134(5) | 13.9020(12) | 12.5404(5) | 14.2645(8) |
| $c$, Å | 15.670(5) | 16.7287(14) | 17.3718(7) | 17.2149(9) |
| $\alpha$, deg | 94.504(5) | 84.964(4) | 86.752(2) | 80.906(3) |
| $\beta$ | 93.034(5) | 79.137(4) | 75.499(2) | 85.682(3) |
| $\gamma$ | 115.329(5) | 73.210(4) | 81.402(2) | 81.442(3) |
| $V$, Å | 2258.7(15) | 2504.4(4) | 2458.76(17) | 2888.9(3) |
| $Z$ | 2 | 2 | 2 | 2 |
| $d_{calc}$, g cm$^{-3}$ | 1.477 | 1.641 | 1.622 | 1.482 |
| $\mu$ (mm$^{-1}$) | 0.631 | 0.742 | 0.650 | 0.471 |
| λ (Å) | 0.71073 | 0.71073 | 0.71073 | 0.71073 |
| $R$[a] | 0.0332 | 0.0525 | 0.0654 | 0.0389 |
| $R_w$ | 0.0919 | 0.1262 | 0.1982 | 0.0982 |

[a] $R = \sum(|F_o| - |F_c|)/\sum|F_o|$, $R_w = [\sum w(|F_o| - |F_c|)^2/\sum w|F_o|^2]^{1/2}$ (based on reflections with $I > 2\sigma(I)$).

observed in the structure of $[RuCl(PPh_3)_2(Tpms)]$ [25]. The Ru–N bond lengths of pyrazolyl ligand in **2**, **6** and **8** complexes which are *trans* to the phosphorus ligands ($PPh_3$) are slightly longer than the other Ru–N bond which is *trans* to OTf, $H_2O$ or $CH_3CN$ ligand. This might indicate the *trans* influence of $PPh_3$ ligand. The P1–Ru–P2 bond angle in all the four structures was found to be about 100°, which is a consequence of the steric bulk of $PPh_3$ ligands. The Ru–H bond length in **1** is 1.58(3) Å which sits comfortably within the range of distances generally observed in the hydride complexes [30]. In complex **2**, the Ru–O bond length is 2.198(2) Å which is longer than that in $[Ru(Cp^*)(OTf)(P^iPr_3)]$ [31] (2.136(2) Å) and shorter than that in $[Ru(SO_3CF_3)\{C_6H_3(CH_2NMe_2)_2\text{-}2,6\}(C_7H_8)]$ [32] complex (2.2327(16) Å).

## Conclusions

In an attempt to stabilize and gain insights into the bonding nature and reactivity behavior of various sigma ligands on a ruthenium center $[Ru(\eta^2\text{-}HX)(Tpms)(PPh_3)_2][OTf]$, (X = H, SiR (R = $Me_3$ or $Me_2Ph$) and $CH_3$), we followed two strategies to generate these complexes in solution. In the first strategy, reaction of $[RuH(Tpms)(PPh_3)_2]$ complex, **1** with electrophilic reagent HOTf results in dihydrogen complex $[Ru(\eta^2\text{-}H_2)(Tpms)(PPh_3)_2][OTf]$ **3**, whereas the reaction of **1** with $Me_3SiOTf$ afforded the dihydrogen complex **3** and complex **1** through an unobserved σ–silane intermediate. In addition, reaction of **1** with $CH_3OTf$ resulted in $[Ru(OTf)(Tpms)(PPh_3)_2]$ complex **2** and free methane through an unobserved sigma methane species. In the second strategy, reaction of $[Ru(OTf)(Tpms)(PPh_3)_2]$ complex, **2** with $H_2$, $PhMe_2SiH$ and $CH_4$ at low temperature were carried out. These reactions resulted in dihydrogen complex, a probable σ–silane complex, and no reaction between complex **2** and methane, respectively.

## Experimental section

### *General procedures*

All reactions were carried out under $N_2$ or Ar using standard Schlenk and inert atmosphere techniques unless otherwise specified [33,34]. Reagent-grade solvents were dried and distilled under $N_2$ atmosphere from Na-benzophenone (hexane, petroleum ether, THF, diethyl ether) just before use. Dichloromethane was first dried and distilled using $P_2O_5$ and once again dried and distilled over $CaH_2$. Solvents for the reactions that involved the synthesis of ruthenium complexes were thoroughly saturated with Ar or $N_2$ just before use. The $^1H$ and $^{31}P$ NMR spectral data were obtained using an Avance Bruker 400 MHz instrument. All chemical shifts are reported on the δ scale. The chemical shift of the residual protons of the deuterated solvent was used as an internal reference. Dichloromethane-$d_2$ ($CD_2Cl_2$) was purchased from Cambridge-Isotopes Limited, USA and distilled over $CaH_2$ prior to use. Methanol was dried and distilled under $N_2$ atmosphere from Na. Variable-temperature $^1H$ $T_1$ measurements were carried out at 400 MHz using the inversion recovery method (180°–τ–90° pulse sequence at each temperature) [35]. All $^{31}P$ NMR spectra were proton-decoupled, unless otherwise stated. $^{31}P$ NMR chemical shifts have been measured relative to 85% $H_3PO_4$ (external) in $CD_2Cl_2$. Lithium tris(pyrazolyl)methane sulfonate (LiTpms) and $[RuH_2(PPh_3)_4]$, $[RuCl(Tpms)(PPh_3)_2]$ complexes were prepared using literature procedures. [10,25,36].

### *X-ray structure determination of **1**, **2**, **6**, and **8***

Good quality crystals of complexes **1**, **2**, **6**, and **8** suitable for X-ray diffraction study were carefully selected after examination under an optical microscope and mounted on the Goniometer head with paraffin oil coating. The unit cell parameters and intensity data were collected at room temperature and 100 K using a Bruker SMART APEX CCD diffractometer equipped with a fine focus Mo Kα X-ray source (50 kV, 40 mA). The data acquisition was done using SMART software and SAINT software was used for data reduction [37]. The empirical absorption corrections were made using the SADABS program [38]. The structure was solved and refined using the SHELXL-97 program [39]. The ruthenium atom was located from the Patterson map, and the non-hydrogen atoms and the hydride were located from the difference Fourier map and refined anisotropically. All other hydrogen atoms were fixed in idealized positions and refined in a riding model.

### *Synthesis of $[RuH(Tpms)(PPh_3)_2]$, **1***

$[RuH_2(PPh_3)_4]$ (0.400 g, 0.347 mmol) and LiTpms (0.102 g, 0.347 mmol) were dissolved in 20 mL of THF. The resulting yellow solution was refluxed for 2 h to give a yellowish green suspension. The mixture was filtered off and the filtrate was concentrated under vacuum and washed with diethyl ether and then finally dried under vacuum to obtain a yellow powder. Pure product of $[RuH(Tpms)(PPh_3)_2]$, **1** was obtained by recrystallization of the residue from dichloromethane/*n*-hexane at room temperature for overnight. Yield: 0.159 g, 50%. Anal. Calcd for $C_{47}H_{45}Cl_2N_6O_3P_2RuS$: C, 56.01; H, 4.50; N, 8.34; S, 3.18. Found: C, 56.59; H, 4.28; N, 8.0; S, 3.17. $^1H$ NMR (400 MHz, $CD_2Cl_2$, 25 °C): δ −13.35 (t, $^2J(HP) = 27.7$ Hz, 1H, Ru–*H*), 5.68 [t, 2H, $H^4(pz')$], 5.98 [t, 1H, $H^4(pz)$], 6.45 [d, 1H, $H^5(pz)$], 6.92 [d, 2H, $H^5(pz')$], 7.02–7.26 [m, 30H, $PC_6H_5$], 8.74 [d, 2H, $H^3(pz')$], 9.05 [d, 1H, $H^3(pz)$] (pz = pyrazolyl group trans to hydride, pz′ = pyrazolyl group trans to $PPh_3$, all coupling constants for pyrazolyl proton resonance were about 2.5 Hz). $^{31}P\{^1H\}$ NMR (161.70 MHz, $CD_2Cl_2$, 25 °C): δ 65.8 (s).

### *Preparation of $[Ru(OTf)(Tpms)(PPh_3)_2]$, **2***

$[RuCl(Tpms)(PPh_3)_2]$ (0.200 g, 0.209 mmol) and AgOTf (0.052 g, 0.209 mmol) were dissolved in 20 mL of dichloromethane. The yellow solution was stirred at room temperature for 30 min to give a yellow suspension. The mixture was filtered through Celite and washed with hexane and dried under vacuum to give a yellow powder of $[Ru(OTf)(Tpms)(PPh_3)_2]$, **2**. Yield: 0.180 g, 80%. Anal. Calcd for $C_{47}H_{43}F_3N_6O_6P_2RuS_2\cdot 2CH_2Cl_2$: C, 47.54; H, 3.50; N, 6.79; S, 5.18. Found: C, 47.32; H, 3.32; N, 6.58; S, 5.14. $^1H$ NMR (400 MHz, $CD_2Cl_2$, 293 K): 5.06 [d, 1H, $H^3(pz)$]; 5.36 [t, 2H, $H^4(pz')$]; 5.90 [t, 2H, $H^4(pz)$]; 7.24 [d, 2H, $H^5(pz')$]; 6.99–7.34 [m, 30H, $P(C_6H_5)_3$]; 8.96 [d, 2H, $H^3(pz')$]; 9.10 [d, 1H, $H^5(pz)$] (pz = pyrazolyl group trans to OTf, pz′ = pyrazolyl group trans to $PPh_3$; all coupling constants for pyrazolyl proton resonance were about 2.5 Hz). $^{31}P\{^1H\}$ NMR (161.70 MHz, $CDCl_3$, 293 K): δ 36.6 (s). $^{19}F$ NMR (376 MHz, $CDCl_3$, 293 K): δ −76.69 (s, 3F). EI-MS $m/z$ = 919[M-OTf].

### *Protonation of $[RuH(Tpms)(PPh_3)_2]$, **1***

$[RuH(Tpms)(PPh_3)_2]$ (0.020 g, 0.021 mmol) was dissolved in 0.5 mL of $CD_2Cl_2$ in a 5 mm NMR tube that was capped with a septum. The resulting solution was subjected to three cycles of freeze–pump–thaw degassing. The tube was cooled to 243 K. One equivalent (ca. 2 μL, 0.028 mmol) of HOTf was added to this solution immediately and then the sample was inserted into the NMR probe, which was pre-cooled to 243 K. The $^1H$ and $^{31}P$ NMR spectra recorded at 243 K showed the presence of the dihydrogen complex **3**. $^1H$ NMR (400 MHz, $CD_2Cl_2$, 243 K): δ −7.63 [br s, 2H, Ru-($H_2$)]; 5.90 [t, 1H, $H^4(pz)$; 5.94 [t, 2H, $H^4(pz')$]; 6.16 [d, 1H, $H^5(pz)$; 6.74 [d, 2H, $H^5(pz')$]; 7.11–7.71 (m, 30H, $PC_6H_5$); 9.04 [d, 2H, $H^3(pz')$]; 9.25

[d, 1H, $H^3$(pz)] (pz = pyrazolyl group trans to $\eta^2$-$H_2$, pz′ = pyrazolyl group trans to $PPh_3$; all coupling constants for pyrazolyl proton resonance were about 2.5 Hz). $^{31}P\{^1H\}$ NMR (161.70 MHz, $CD_2Cl_2$, 243 K): $\delta$ 43.6 (s). Variable-temperature $T_1$ measurements on the $H_2$ signal were carried out by the inversion-recovery method using standard 180°−τ−90° pulse sequence. $T_1$ (400 MHz, ms): 21.6 (193 K), 20.9 (203 K), 18.7 (213 K), 18.0 (223 K), 17.3 (233 K), 15.8 (243 K), 18.0 (253 K), 18.7 (263 K), 19.4 (273 K), 19.4 (283), 20.2 (293 K). $T_1$(min) (400 MHz, 243 K): 15.8 ms.

*Preparation of [Ru(HD)(Tpms)(PPh$_3$)$_2$][OTf]*

In an attempt to prepare the HD isotopomer of [Ru($\eta^2$-$H_2$)(Tpms)($PPh_3$)$_2$][OTf], we purged the corresponding $CD_2Cl_2$ solution containing the [Ru($\eta^2$-$H_2$)(Tpms)($PPh_3$)$_2$][OTf] complex with HD gas (generated from NaH and $D_2O$) at 243 K. The $^1H$ NMR spectrum of the resulting solution was then recorded at 243 K. The $\eta^2$-HD signal ($\delta$ −7.6 (tt), $^1J$(HD) = 31.6 Hz, $^2J$(HP) = 6.6 Hz) was observed after nullifying the $\eta^2$-$H_2$ peak at $\delta$ −7.6 using the inversion-recovery method with a delay time of 11 ms.

*Reaction of complex **1** with Me$_3$SiOTf*

This reaction was carried out using complex **1** (0.02 g, 0.021 mmol) and $Me_3SiOTf$ (8 μL, 0.043 mmol). The sealed NMR tube with the frozen contents was inserted into the NMR probe precooled to 183 K and the $^1H$ and $^{31}P\{^1H\}$ spectra were recorded as the reaction progressed upon raising the temperature. In this case we noted the formation of free $Me_3SiOH$ along with [Ru($\eta^2$-$H_2$)(Tpms)($PPh_3$)$_2$]. $^1H$ NMR (400 MHz, $CD_2Cl_2$, 193−293 K): $\delta$ 0.05 ppm [1H, $Me_3SiOH$].

*Attempt to prepare [Ru($\eta^2$-CH$_4$)(Tpms)(PPh$_3$)$_2$][OTf]*

A flame-dried 5 mm Schlenk NMR tube was charged with [RuH(Tpms)($PPh_3$)$_2$] (0.020 g, 0.021 mmol) and ca. 0.5 mL of $CD_2Cl_2$ was added under nitrogen. The sample was cooled to 77 K, and then $CH_3OTf$ (4 μL, 0.036 mmol) was added and the tube was sealed under vacuum. The sample was then inserted into the NMR probe immediately, which was pre-cooled to 183 K. The progress of the reaction was monitored by recording the $^1H$ and $^{31}P$ NMR spectra of the sample over a temperature range 203−298 K. The $^1H$ and $^{31}P\{^1H\}$ NMR spectra recorded at 213 K showed the presence of free methane, [Ru(OTf)(Tpms)($PPh_3$)$_2$], **2** and [Ru($OH_2$)(Tpms)($PPh_3$)$_2$], **6** complexes. $^1H$ NMR ($CD_2Cl_2$, 213 K): $\delta$ 0.18 (s, 4H, $CH_4$).

*Reaction of RuH(Tpms)(PPh$_3$)$_2$ complex **1** with CD$_3$OTf*

This reaction was conducted in a similar manner to that of complex **1** with $CH_3OTf$ starting with complex **1** (0.020 g, 0.021 mmol) and $CD_3OTf$ (ca. 4 μL, 0.030 mmol). The sealed NMR tube with the frozen contents was inserted into the NMR probe precooled to 213 K and the $^1H$ and $^{31}P\{^1H\}$ NMR spectra were recorded as the reaction progressed upon raising the temperature. In this case we found free $CD_3H$ along with [Ru(OTf)(Tpms)($PPh_3$)$_2$], **2** and [Ru($OH_2$)(Tpms)($PPh_3$)$_2$], **6** complexes. $^1H$ NMR ($CD_2Cl_2$, 213−293 K): $\delta$ 0.16 (sept, 1H, $CD_3H$).

*Reaction of [Ru(OTf)(Tpms)(PPh$_3$)$_2$] with H$_2$ at 298 K*

Complex **1** (0.020 g, 0.018 mmol) was dissolved in 0.6 mL of $CD_2Cl_2$ in a 5 mm high pressure NMR tube. Next, $H_2$ (2 atm) was pressurized for a period of 5 min. The $^1H$ and the $^{31}P$ NMR spectra of the sample recorded immediately thereafter at 298 K showed the formation of [Ru($\eta^2$-$H_2$)(Tpms)($PPh_3$)$_2$][OTf], **3** complex (5%) along with starting material.

*Reaction of [Ru(OTf)(Tpms)(PPh$_3$)$_2$] with PhMe$_2$SiH*

Complex **2** (0.020 g, 0.018 mmol) was dissolved in 0.6 mL of $CD_2Cl_2$ in a 5 mm NMR tube and then the tube was cooled to 203 K using slush bath (ethanol/liq $N_2$). Next, 1 equiv of $Me_2PhSiH$ (3 μL, 0.018 mmol) was added at 203 K, immediately the sample was inserted into the NMR probe, which was pre-cooled to 203 K. The $^1H$ and $^{31}P\{^1H\}$ NMR spectra were recorded. The same reaction was also carried out at room temperature and the products were characterized by NMR spectroscopy.

*Reaction of [Ru(OTf)(Tpms)(PPh$_3$)$_2$] complex **2** with methane (7 bar) in a pressure-stable NMR tube*

Complex **2** (0.020 g, 0.018 mmol) was dissolved in 0.6 mL of $CD_2Cl_2$ in a high-pressure NMR tube. The solution was subjected to one freeze−pump−thaw degassing cycle, and then $CH_4$ (7 bar) was pressurized in the tube. The tube was closed by a Teflon valve, and the progress of the reaction was monitored by using VT NMR spectroscopy. $^1H$ NMR spectroscopy did not reveal the formation of the [Ru($\eta^2$-$CH_4$)(Tpms)($PPh_3$)$_2$][OTf] σ−methane complex.

*Preparation of [Ru(L′)(Tpms)(PPh$_3$)$_2$][OTf] (L′ = H$_2$O(6), CH$_3$CN(8))*

[Ru(OTf)(Tpms)($PPh_3$)$_2$] (0.1 g, 0.092 mmol) and $H_2O$ (ca. 10 μL, 0.140 mmol) were dissolved in 10 mL of dichloromethane under nitrogen atmosphere. The yellow solution was stirred at room temperature for 5 min to give a light yellow solution. The yellow product of [Ru($H_2O$)(Tpms)($PPh_3$)$_2$][OTf] was obtained in a yield of 75 mg, 70%. $^1H$ NMR (400 MHz, $CDCl_3$, 293 K): 5.43 [d, 1H, $H^5$(pz)]; 5.59 [t, 1H, $H^4$(pz)]; 5.72 [t, 2H, $H^4$(pz′)]; 6.21[d, 2H, $H^5$(pz′)]; 7.11−7.89 [m, 30H, P($C_6H_5$)$_3$]; 8.78 [d, 2H, $H^3$(pz′)]; 9.23 [d, 1H, $H^3$(pz)] (pz = pyrazolyl group trans to $H_2O$, pz′ = pyrazolyl group *trans* to $PPh_3$; all coupling constants for pyrazolyl proton resonance were about 2.5 Hz). $^{31}P\{^1H\}$ NMR (161.70 MHz, $CD_2Cl_2$, 293 K): $\delta$ 39.9 (s). [Ru($NCCH_3$)(Tpms)($PPh_3$)$_2$][OTf] compound was prepared using above similar procedure. $^1H$ NMR (400 MHz, $CDCl_3$, 293 K): 2.71 (s, 3H, $CH_3CN$), 5.52 [t, 1H, $H^4$(pz); 5.98 [t, 2H, $H^4$(pz′)]; 6.52 [d, 1H, $H^5$(pz)]; 6.74 [d, 2H, $H^5$(pz′)]; 6.95−7.42 [m, 30H, P($C_6H_5$)$_3$]; 8.94 [d, 2H, $H^3$(pz′)]; 9.16 [d, 1H, $H^3$(pz)] (pz = pyrazolyl group *trans* to $NCCH_3$, pz′ = pyrazolyl group *trans* to $PPh_3$; all coupling constants for pyrazolyl proton resonance were about 2.5 Hz). $^{31}P\{^1H\}$ NMR (161.70 MHz, $CD_2Cl_2$, 293 K): $\delta$ 39.1 (s).

## Appendix A. Supplementary material

CCDC 984250−984253 contain the supplementary crystallographic data for [RuH(Tpms)($PPh_3$)$_2$] (**1**), [Ru(OTf)(Tpms)($PPh_3$)$_2$] (**2**), [Ru($H_2O$)(Tpms)($PPh_3$)$_2$] (**6**) and [Ru($CH_3CN$)(Tpms)($PPh_3$)$_2$] (**8**). These data can be obtained free of charge from The Cambridge Crystallographic Data Centre via www.ccdc.cam.ac.uk/data_request/cif.

## Appendix B. Supplementary data

Supplementary data related to this article can be found at http://dx.doi.org/10.1016/j.jorganchem.2014.03.027.

## References

[1] G.J. Kubas, in: Metal Dihydrogen and σ-Bond Complexes, Kluwer Academic/Plenum Publishers, New York, 2001.

[2] G.S. McGrady, G. Guilera, Chem. Soc. Rev. 32 (2003) 383–392.
[3] R.H. Crabtree, Angew. Chem. Int. Ed. Engl. 32 (1993) 789–805.
[4] G. Alcaraz, S. Sabo-Etienne, Coord. Chem. Rev. 252 (2008) 2395–2409.
[5] C. Hall, R.N. Perutz, Chem. Rev. 96 (1996) 3125–3146.
[6] W.H. Bernskoetter, C.K. Schauer, K.I. Goldberg, M. Brookhart, Science 326 (2009) 553–556.
[7] D.J. Lawes, S. Geftakis, G.E. Ball, J. Am. Chem. Soc. 127 (2005) 4134–4135.
[8] S.D. Pike, A.L. Thompson, A.G. Algarra, D.C. Apperley, S.A. Macgregor, A.S. Weller, Science 337 (2012) 1648–1651.
[9] S. Trofimenko, Chem. Rev. 93 (1993) 943–980.
[10] W. Kläui, M. Berghahn, G. Rheinwald, H. Lang, Angew. Chem. Int. Ed. 39 (2000) 2464–2466.
[11] W. Kläui, M. Berghahn, W. Frank, Guido J. Reiß, T. Schönherr, G. Rheinwald, H. Lang, Eur. J. Inorg. Chem. 2003 (2003) 2059–2070.
[12] W. Kläui, D. Schramm, W. Peters, Eur. J. Inorg. Chem. 2001 (2001) 3113–3117.
[13] S. Miguel, J. Diez, M.P. Gamasa, M.E. Lastra, Eur. J. Inorg. Chem. 2011 (2011) 4745–4755.
[14] G.J. Kubas, Chem. Rev. 107 (2007) 4152–4205.
[15] E. Scharrer, S. Chang, M. Brookhart, Organometallics 14 (1995) 5686–5694.
[16] X.-L. Luo, G.J. Kubas, J.C. Bryan, C.J. Burns, C.J. Unkefer, J. Am. Chem. Soc. 116 (1994) 10312–10313.
[17] W.-C. Chan, C.-P. Lau, Y.-Z. Chen, Y.-Q. Fang, S.-M. Ng, G. Jia, Organometallics 16 (1997) 34–44.
[18] P.J. Desrosiers, L. Cai, Z. Lin, R. Richards, J. Halpern, J. Am. Chem. Soc. 113 (1991) 4173–4184.
[19] dHH(Å) = 1.44 − 0.0168[J(H,D)].
[20] T.A. Luther, D.M. Heinekey, J. Am. Chem. Soc. 119 (1997) 6688–6689.
[21] X.L. Luo, R.H. Crabtree, J. Am. Chem. Soc. 111 (1989) 2527–2535.
[22] J.A. Calladine, S.B. Duckett, M.W. George, S.L. Matthews, R.N. Perutz, O. Torres, K.Q. Vuong, J. Am. Chem. Soc. 133 (2011) 2303–2310.
[23] R.D. Young, A.F. Hill, W. Hillier, G.E. Ball, J. Am. Chem. Soc. 133 (2011) 13806–13809.
[24] T.Y. Lee, L. Dang, Z. Zhou, C.H. Yeung, Z. Lin, C.P. Lau, Eur. J. Inorg. Chem. 2010 (2010) 5675–5684.
[25] K. Hindson, Eur. J. Inorg. Chem. 2011 (2011) 4–6.
[26] J.Y. Corey, J. Braddock-Wilking, Chem. Rev. 99 (1999) 175–292.
[27] J. Huhmann-Vincent, B.L. Scott, G.J. Kubas, Inorg. Chim. Acta 294 (1999) 240–254.
[28] H.F.T. Klare, M. Oestreich, J.-i. Ito, H. Nishiyama, Y. Ohki, K. Tatsumi, J. Am. Chem. Soc. 133 (2011) 3312–3315.
[29] Y.-Z. Chen, W.C. Chan, C.P. Lau, H.S. Chu, H.L. Lee, G. Jia, Organometallics 16 (1997) 1241–1246.
[30] K. Abdur-Rashid, R. Abbel, A. Hadzovic, A.J. Lough, R.H. Morris, Inorg. Chem. 44 (2005) 2483–2492.
[31] M.E. Fasulo, P.B. Glaser, T.D. Tilley, Organometallics 30 (2011) 5524–5531.
[32] J.-P. Sutter, S.L. James, P. Steenwinkel, T. Karlen, D.M. Grove, N. Veldman, W.J.J. Smeets, A.L. Spek, G. van Koten, Organometallics 15 (1996) 941–948.
[33] S. Herzog, J. Dehnert, K. Luhder, in: Techniques of Inorganic Chemistry, Interscience, New York, 1969.
[34] D.F. Shriver, M.A. Drezdon, in: The Manipulation of Air-sensitive Compounds, Wiley, New York, 1986.
[35] D.G. Hamilton, R.H. Crabtree, J. Am. Chem. Soc. 110 (1988) 4126–4133.
[36] J.J. Levison, S.D. Robinson, J. Chem. Soc. A Inorg. Phys. Theor. (1970) 2947–2954.
[37] Siemens Analytical X-ray Instruments, Inc., WI, Madison, 1995.
[38] G.M. Sheldrick, in: SADABS User Guide, University of Göttingen, Göttingen, Germany, 1993.
[39] G.M. Sheldrick, Acta Cryst. Found. Crystallogr. 64 (2008) 112–122.